

Black-box Backdoor Defense via Zero-shot Image Purification

Yucheng Shi,[†] Mengnan Du,[‡] Xuansheng Wu,[†] Zihan Guan,[†] Ninghao Liu[†]

[†]School of Computing, University of Georgia, Athens, GA

[‡]Department of Data Science, New Jersey Institute of Technology, Newark, NJ

{yucheng.shi, xuansheng.wu, zihan.guan, ninghao.liu}@uga.edu, mengnan.du@njit.edu

Abstract

Backdoor attacks inject poisoned data into the training set, resulting in misclassification of the poisoned samples during model inference. Defending against such attacks is challenging, especially in real-world black-box settings where only model predictions are available. In this paper, we propose a novel backdoor defense framework that can effectively defend against various attacks through zero-shot image purification (ZIP). Our proposed framework can be applied to black-box models without requiring any internal information about the poisoned model or any prior knowledge of the clean/poisoned samples. Our defense framework involves a two-step process. First, we apply a linear transformation on the poisoned image to destroy the trigger pattern. Then, we use a pre-trained diffusion model to recover the missing semantic information removed by the transformation. In particular, we design a new reverse process using the transformed image to guide the generation of high-fidelity purified images, which can be applied in zero-shot settings. We evaluate our ZIP backdoor defense framework on multiple datasets with different kinds of attacks. Experimental results demonstrate the superiority of our ZIP framework compared to state-of-the-art backdoor defense baselines. We believe that our results will provide valuable insights for future defense methods for black-box models.

1 Introduction

As machine learning becomes increasingly integrated into high-stakes applications such as healthcare [20], finance [11], and autonomous systems [27], ensuring the security and reliability of these models has become more critical, which includes defending against various backdoor attacks [6, 3, 19]. The backdoor attack is a type of attack on machine learning models in which an attacker can manipulate the model behavior by poisoning training data with malicious samples that contain a trigger pattern and a target label, or altering the weights of the model [15]. Although several defense strategies have been proposed in recent years to mitigate the effects of backdoor attacks, many of them require access to the model’s internal structure and poisoned training data [15]. This is not always feasible in real-world black-box settings, as users are unable to check or audit the inner workings of the model. For example, end-users may prefer to use pre-trained models provided by third-party vendors, such as those available on AWS SageMaker [1] or Microsoft Azure Machine Learning [2], to save on computation costs. However, they also lose control over the model training or deploying processes. In such cases, backdoor attacks can be particularly harmful and hard to detect because the end-user can only access prediction results. This lack of transparency poses a significant challenge for detecting and defending against black-box backdoor attacks.

Existing defense methods for black-box backdoor models fall into two categories. The first type trains a detection model with clean/poisoned images as inputs [25, 7, 14, 5]. However, this method has limitations such as being dependent on the quality and quantity of collected data, and not being able to use the detected poisoned images for further analysis [7, 25, 5]. The second type applies strong image transformations during the inference stage before feeding poisoned images to the poisoned model [17, 26]. This kind of methods can defend against static pattern-based attacks, but are not effective against advanced attacks with advanced patterns [17]. Both methods have limitations and are not effective in real-world applications. To overcome the limitations of existing black-box backdoor defense methods, we aim to propose a novel defense framework that does not require (1) any internal information of the classification model or (2) any prior knowledge of the clean/poisoned samples. And our proposed method can help benign end-users utilize those poisoned samples that are maliciously attacked by attackers, rather than discarding them. However, we face two main challenges in designing such a framework.

(1) **Trade-off between image transformation and fidelity.** Strong transformation is needed to create a mismatch between advanced trigger patterns and poisoned labels. But it can also remove

important semantic information from the images. Since the transformation-based defense method applies the transformation to the entire dataset, it can cause the classification accuracy (CA) to drop on the clean images. To avoid such drop, we need to maintain a high fidelity of the transformed image while we destroy the trigger pattern. One potential solution to solve this is to recover the missing information removed by strong transformation. However, how to recover the semantic information instead of the trigger pattern from transformed images remains a challenge.

(2) **Defending against attacks in a zero-shot setting.** In our proposed framework, we define "zero-shot" as the ability to defend against various attacks without relying on any prior knowledge of the clean or poisoned image samples. In other words, our approach does not require access to any clean or poisoned image samples and can be applied directly to unseen attack scenarios. This setting is crucial because real-world users have limited information, while new threats always emerge. Collecting the most recent attacked images for the detection models' training samples may not be feasible. Therefore, effectively defending against poisoned images without any reference samples poses a significant challenge.

To address the above challenges, we propose a novel backdoor defense framework that can effectively defend against various attacks through Zero-shot Image Purification (ZIP). The purification in our ZIP framework aims to preserve the original image's semantic information while minimizing the presence of the trigger pattern. To achieve this goal, we first utilize image transformation techniques to destruct the trigger pattern. We then leverage an off-the-shelf, pre-trained diffusion generative model to restore the transformed semantic information. Our defense strategy is based on the motivation that the semantic information in a poisoned image (e.g., human faces, cars) constitutes the majority of the image and typically falls within the pre-training data distribution. Conversely, the trigger pattern (e.g., small white box, colorful spirals) is inconspicuous and not included in the pre-training datasets. Since the diffusion model can only sample images from the training dataset distribution [9], purified images generated from the diffusion model can only retain their semantic information instead of the trigger pattern. As a result, our purification approach can effectively defend against various attacks while maintaining high-fidelity in the restored images. Our main contributions are summarized as follows.

- We develop a novel defense framework that can be applied to black-box models without requiring any internal information about the model. Our defense system is also model-agnostic, making it versatile and easy to use with various models without retraining.
- Our proposed framework is designed to function in a zero-shot setting, meaning it can operate without requiring any prior knowledge of the clean or poisoned images. This feature relieves end-users from the need to collect samples, which enhances the framework's application ability and usability.
- Our defense framework is capable of achieving decent classification accuracy on the purified images that are originally poisoned samples, even with an attack model as the classifier. This improvement further enhances the framework's effectiveness and practicality.

2 Preliminaries

2.1 Diffusion Model

The denoising diffusion probabilistic model (DDPM [9]) is a generative model that has recently gained attention due to its ability to generate high-quality images. The original DDPM includes two processes: the forward process and the reverse process. In the forward process, the model iteratively adds noise to the input image until it transforms to random Gaussian noise \mathbf{x}_T , then in the reverse process, the model iteratively removes the added noise from the Gaussian noise image \mathbf{x}_T to generate a noise-free image \mathbf{x}_0 . The generated image \mathbf{x}_0 fits the distribution of the input images in the forward process. The model details are as follows:

Forward Process: In the forward process, a noise-free image \mathbf{x}_0 is transformed to a noisy image \mathbf{x}_t with controlled noise. Specifically, Gaussian noise ϵ is gradually added to image \mathbf{x}_0 in T steps based on the variance schedule β_t :

$$q(\mathbf{x}_t | \mathbf{x}_{t-1}) := \mathcal{N}(\mathbf{x}_t; \sqrt{1 - \beta_t} \mathbf{x}_{t-1}, \beta_t \mathbf{I}), \quad (1)$$

A nice property of the above process is that we can sample noised image at step t using reparameterization trick:

$$q(\mathbf{x}_t | \mathbf{x}_0) = \mathcal{N}(\mathbf{x}_t; \sqrt{\bar{\alpha}_t} \mathbf{x}_0, (1 - \bar{\alpha}_t) \mathbf{I}), \quad \mathbf{x}_t = \sqrt{\bar{\alpha}_t} \mathbf{x}_0 + \sqrt{1 - \bar{\alpha}_t} \epsilon, \quad \epsilon \sim \mathcal{N}(0, \mathbf{I}), \quad (2)$$

where we have $\alpha_t = 1 - \beta_t$ and $\bar{\alpha}_t = \prod_{i=1}^t \alpha_i$.

Reverse Process: In the reverse process, the noisy input image \mathbf{x}_T obtained from the forward stage is transformed into a noise-free output image \mathbf{x}_0 step by step. In each step, the diffusion model takes in the current image state \mathbf{x}_t and produces a previous state \mathbf{x}_{t-1} . We aim to obtain clean images \mathbf{x}_0 by iteratively sampling \mathbf{x}_{t-1} from $p(\mathbf{x}_{t-1}|\mathbf{x}_t, x_0)$:

$$\mathbf{x}_{t-1} = \frac{\sqrt{\bar{\alpha}_{t-1}}\beta_t}{1 - \bar{\alpha}_t}\mathbf{x}_0 + \frac{\sqrt{\alpha_t}(1 - \bar{\alpha}_{t-1})}{1 - \bar{\alpha}_t}\mathbf{x}_t + \sigma_t\epsilon, \quad \epsilon \sim \mathcal{N}(0, \mathbf{I}), \quad \sigma_t^2 = \frac{1 - \bar{\alpha}_{t-1}}{1 - \bar{\alpha}_t}\beta_t, \quad (3)$$

Based on Equation 2, we can estimate a noisy input image $\mathbf{x}_{0|t}$ based on the step t observation \mathbf{x}_t :

$$\mathbf{x}_{0|t} = \frac{1}{\sqrt{\bar{\alpha}_t}}(\mathbf{x}_t - \sqrt{1 - \bar{\alpha}_t}\epsilon_t), \quad (4)$$

where ϵ_t denotes the estimation of the real ϵ in time step t . In each step t , DDPM utilizes a neural network $g_\phi(\cdot)$ to predict the noise ϵ_t , i.e., $\epsilon_t = g_\phi(\mathbf{x}_t, t)$. With this estimation, we can transform Equation 3 into the following form:

$$\mathbf{x}_{t-1} = \frac{1}{\sqrt{\alpha_t}}(\mathbf{x}_t - \frac{1 - \alpha_t}{\sqrt{1 - \bar{\alpha}_t}}\epsilon_t) + \sigma_t\epsilon. \quad (5)$$

2.2 Notation and Problem Definition

This paper addresses the backdoor defense problem in the context of image classification. The goal of image classification is to learn a function $f_\theta(\mathbf{x})$ that maps input images $\mathbf{x} \in \mathcal{X}$ to their correct labels $y \in \mathcal{Y}$, where \mathcal{X} denotes the set of images, \mathcal{Y} denotes their corresponding labels, and θ represents the parameters of the function f_θ . When this learning process is under attack, an attacker can alter the classification result by modifying a small portion of the training dataset \mathcal{X}^{attack} to insert a "backdoor" into the model. This backdoor is usually a specific pattern \mathbf{p} (or a set of patterns), such as mosaic pixels arranged on a 2×2 grid. When this pattern is present in an input image, it forces the model to generate a predetermined output, regardless of the true label of the image.

The backdoor attack can be formalized as follows: given an original clean image $\mathbf{x} \in \mathcal{X}$ and a trigger pattern \mathbf{p} , simply adding the pattern \mathbf{p} to \mathbf{x} can produce the poisoned image $\mathbf{x}^P = \mathbf{x} + \mathbf{p}$. During the training process, the attackers first obtain poisoned image \mathbf{x}^P to form a subset of the training images \mathcal{X}^{attack} . After training on the \mathcal{X}^{attack} , the attacked classification function is denoted as $f_\theta^{attack}(\mathbf{x})$. During testing, an attacker can apply the same trigger pattern \mathbf{p} to a clean test image \mathbf{x} to create a poisoned image $\mathbf{x}^P = \mathbf{x} + \mathbf{p}$, which will be classified by the backdoored model as the target label $y^{target} = f_\theta^{attack}(\mathbf{x}^P) \neq y$. To defend against the above attack, we formally define our defense problem as follows.

Problem 1. Image Purification for Backdoor Defense. *Our defense will be implemented in the model inference stage. Let f_θ^{attack} denote the attacked neural network that has been trained on poisoned dataset \mathcal{X}^{attack} . In our study, we consider the challenging black-box setting in real-world scenarios, where we lack access to the parameters of the f_θ^{attack} model. Given a poisoned image \mathbf{x}^P , our goal is to remove the effect of trigger pattern \mathbf{p} from \mathbf{x}^P to obtain a purified image \mathbf{x}' . The purified image should be classified as the same type as the original clean image \mathbf{x} , i.e., $f_\theta(\mathbf{x}') = f_\theta(\mathbf{x}) \neq f_\theta(\mathbf{x}^P)$. For the purified image \mathbf{x}' , ideally we have $\mathbf{x}' = \mathbf{x}$.*

Specifically, we propose to conduct the backdoor defense by eliminating trigger patterns in poisoned images through image purification during the model inference stage. This is inspired by this observation that the integrity of trigger patterns is the key for the backdoor attack to mislead the model, while corrupting the trigger pattern will significantly compromise the effectiveness of the attack [17].

3 Proposed Defense Framework

In this section, we present our proposed backdoor defense **ZIP** (Zero-shot Image Purification) which is performed in the zero-shot setting where we lack any prior knowledge of the trigger pattern. Specifically, we utilize the power of an off-the-shelf pre-trained diffusion model to generate high-quality purified images.

3.1 Overview of Proposed Framework

Our proposed defense framework is based on the reverse process of the diffusion model, as illustrated in Figure 1. To reduce computation and eliminate the need for sample training, we leverage an off-the-shelf

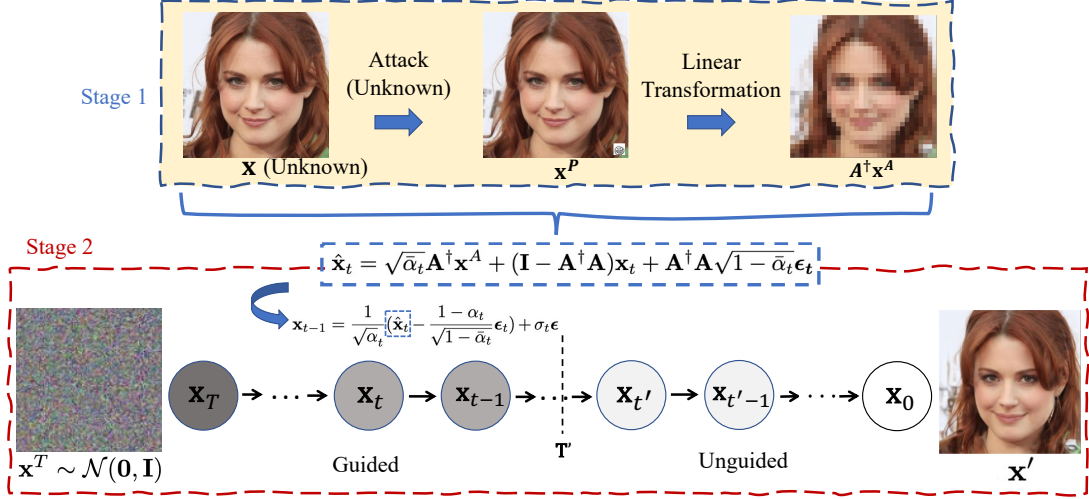


Figure 1: The framework of our **ZIP** backdoor defense. In Stage 1, we use a linear transformation to destruct the trigger pattern in poisoned image \mathbf{x}^P . In Stage 2, we make use of a pre-trained diffusion model to generate a purified image. From time step T to T' : starting from the Gaussian noise image \mathbf{x}^T , we use the transformed image $\mathbf{A}^\dagger \mathbf{x}^A$ obtained in Stage 1 to guide the generation of the purified image. From time step T' to 0 : we discard $\mathbf{A}^\dagger \mathbf{x}^A$ and exclusively use the diffusion model to generate \mathbf{x}' .

pre-trained diffusion model g_ϕ [4]. Our objective is to generate a purified image for a specific image while destroying any trigger patterns. While a vanilla reverse process can generate a noise-free image that fits the distribution of the pre-trained model, the resulting image content cannot be controlled, thus failing to satisfy our high-fidelity requirements. Directly incorporating poisoned images into the reverse process to guide the generation process can produce high-fidelity images but may retain the trigger pattern, thus failing to achieve our purification objectives.

To address these challenges, we first perform a robust image transformation in the poisoned input image to destroy the trigger pattern. However, this operation will also destruct the semantic information and diminish the fidelity, decreasing the classification accuracy. To tackle this problem, we propose utilizing a diffusion model to generate high-quality purified images, and introduce a novel reverse process that is conditional on poisoned images to guide the generation of the purified images. Specifically, we apply the range-null decomposition [22] to extract the transformed image’s deeper relation to the original image, and use this relation as constraint to ensure the generation of high-fidelity purified images. As the trigger pattern is destroyed in the transformed image, it will not be present in the purified image. Moreover, to further mitigate the trigger effect, our framework can switch to the vanilla reverse process in the final stages, where the semantic information in the image is adequate to guide the generation process. In contrast, since the trigger pattern is usually not included in the distribution of pre-trained model, it will not appear in the purified image.

3.2 Image Transformation Constraints

As the first step, we apply image transformation on the poisoned image to destruct the trigger pattern, e.g., by using average pooling to blur poisoned images. Formally, we denote the applied image transformation as a liner operator function \mathbf{A} , and let the transformed image be $\mathbf{x}^A = \mathbf{A}\mathbf{x}^P = \mathbf{A}(\mathbf{x} + \mathbf{p})$. However, directly using the transformed image as the purification result could lead to poor classification accuracy due to fidelity loss induced by \mathbf{A} , which is supported by several previous studies [21]. Recovering the original image \mathbf{x} from the transformed image \mathbf{x}^A is a linear inverse problem that is difficult to solve [12].

To recover the lost information, an intuitive way is to apply an image generative model, e.g., the diffusion model, to yield a purified image with high fidelity. However, images are generated from random Gaussian noise in the diffusion model, which lacks control over the result and cannot be directly applied to solve our problem. Thus, we derive a constraint for the generation process of diffusion models to precisely recover the original image. Specifically, for an ideally purified image \mathbf{x}' , it should satisfy $\mathbf{x}' = \mathbf{x}$, so we establish the constraint as follows:

$$\mathbf{A}(\mathbf{x}' + \mathbf{p}) = \mathbf{A}(\mathbf{x} + \mathbf{p}) = \mathbf{x}^A. \quad (6)$$

Then, we leverage the power of range-null space decomposition (RND) [24, 22] to extract additional relations between \mathbf{x} and \mathbf{x}^A . According to the RND theory, it is possible to decompose an image \mathbf{x} into two parts using a linear operator \mathbf{A} (e.g., average pooling) and its pseudo-inverse \mathbf{A}^\dagger (e.g., upsampling) that satisfies $\mathbf{A}\mathbf{A}^\dagger\mathbf{A} = \mathbf{A}$. The decomposition can be expressed as $\mathbf{x} = \mathbf{A}^\dagger\mathbf{A}\mathbf{x} + (\mathbf{I} - \mathbf{A}^\dagger\mathbf{A})\mathbf{x}$, where the first part represents the observable information in the range-space, and the second part represents the lost information in the null-space removed by transformation¹. Applying this decomposition to Equation 6, we could have:

$$(\mathbf{x}' + \mathbf{p}) = \mathbf{A}^\dagger\mathbf{A}(\mathbf{x}' + \mathbf{p}) + (\mathbf{I} - \mathbf{A}^\dagger\mathbf{A})(\mathbf{x}' + \mathbf{p}). \quad (7)$$

Using this equation, we can derive a constraint as follows for image purification to restore the original \mathbf{x} .

$$\mathbf{x}' = \mathbf{A}^\dagger\mathbf{x}^A - \mathbf{A}^\dagger\mathbf{A}\mathbf{p} + (\mathbf{I} - \mathbf{A}^\dagger\mathbf{A})\mathbf{x}', \quad (8)$$

where we can observe that the ideally purified images are composed of three parts. The first two parts are in the range space: the observable information stored in the transformed image $\mathbf{A}^\dagger\mathbf{x}^A$, as well as the intractable information embedded in the transformed trigger pattern $\mathbf{A}^\dagger\mathbf{A}\mathbf{p}$; and the last part is unobservable in the null-space since it is removed by image transformation. To restore the lost information in the null-space, we utilize the observable information in the range-space as references. This approach will be explained in more detail in Section 3.3. However, it is important to note that the second component mentioned earlier is often difficult to estimate in our zero-shot setting. To address this challenge, we propose an approximation approach that will be introduced in Section 3.4.

3.3 Reverse Process Conditional on Poisoned Images

The reverse process of the diffusion model takes Gaussian noise \mathbf{x}_T as input (see Figure 1), and can generate a noise-free image \mathbf{x}_0 by iteratively removing noise from the input. However, the vanilla reverse process in Section 2.1 generates uncontrollable random images without any further constraints, which does not satisfy the requirement of fidelity. To address this issue, we utilize the image transformation constraint discussed in Equation 8 to encourage the generated image \mathbf{x}_0 to closely match the original image \mathbf{x} . In our setting, we consider the generated noise-free image \mathbf{x}_0 as the purified image \mathbf{x}' , where $\mathbf{x}_0 = \mathbf{x}'$. We also use \mathbf{x}_t to denote the image at time step t in the reverse process of the diffusion model. Specifically, we design a new reverse process conditional on the poisoned image. By combining Equation 4 and Equation 8, we can derive the constraints for the intermediate state \mathbf{x}_t as follows:

$$\mathbf{x}_t = \sqrt{\bar{\alpha}_t}\mathbf{A}^\dagger\mathbf{x}^A - \sqrt{\bar{\alpha}_t}\mathbf{A}^\dagger\mathbf{A}\mathbf{p} + (\mathbf{I} - \mathbf{A}^\dagger\mathbf{A})\mathbf{x}_t + \mathbf{A}^\dagger\mathbf{A}\sqrt{1 - \bar{\alpha}_t}\boldsymbol{\epsilon}_t, \quad (9)$$

where $\boldsymbol{\epsilon}_t$ denotes the estimated noise, which is calculated using the pre-trained diffusion model g_ϕ : $\boldsymbol{\epsilon}_t = g_\phi(\mathbf{x}_t, t)$. The above constraints indicate that any ideally purified images at each time step t should comply with this constraint.

Next, we modify the original reverse process in Equation 5 to accommodate this constraint. The modified reverse process can be transformed as:

$$\mathbf{x}_{t-1} = \frac{1}{\sqrt{\alpha_t}}(\sqrt{\bar{\alpha}_t}\mathbf{A}^\dagger\mathbf{x}^A - \sqrt{\bar{\alpha}_t}\mathbf{A}^\dagger\mathbf{A}\mathbf{p} + (\mathbf{I} - \mathbf{A}^\dagger\mathbf{A})\mathbf{x}_t + \mathbf{A}^\dagger\mathbf{A}\sqrt{1 - \bar{\alpha}_t}\boldsymbol{\epsilon}_t - \frac{1 - \alpha_t}{\sqrt{1 - \alpha_t}}\boldsymbol{\epsilon}_t) + \sigma_t\boldsymbol{\epsilon}, \quad (10)$$

It is worth noting that the above reverse process will be applied to all test images, regardless of whether they are attacked or not. The generated image after this reverse process can preserve the semantic information in the clean image and helps maintain a high classification accuracy.

3.4 Approximation of \mathbf{x}_t in the Zero-shot Setting

In this section, we present an approximation of Equation 10 to address the practical challenges of applying it directly in the zero-shot and black-box settings. In these scenarios, the trigger pattern used to poison the image is unknown and designed to be subtle to evade detection by end-users without access to the training data or model internal information. Therefore, to address this issue, we propose to omit the trigger pattern from the decomposition equation when its contribution is negligible compared to other components. Our proposed approximated form is presented below:

$$\hat{\mathbf{x}}_t = \sqrt{\bar{\alpha}_t}\mathbf{A}^\dagger\mathbf{x}^A + (\mathbf{I} - \mathbf{A}^\dagger\mathbf{A})\mathbf{x}_t + \mathbf{A}^\dagger\mathbf{A}\sqrt{1 - \bar{\alpha}_t}\boldsymbol{\epsilon}_t, \quad (11)$$

¹Usually, we have $\mathbf{A}^\dagger\mathbf{A} \neq \mathbf{I}$, which implies that this operation is lossy. When applying $\mathbf{A}^\dagger\mathbf{A}$ to an image, certain information will be removed, making this operation irreversible.

Algorithm 1 Zero-shot Image Purification (with DDPM)

Require: Poisoned image \mathbf{x}^P ; liner transformation \mathbf{A} and its pseudo-inverse \mathbf{A}^\dagger ; pre-trained diffusion model g ; hyperparameter λ .

Ensure: $\mathbf{x}^A = \mathbf{A}\mathbf{x}^P$, $T' = \lambda T$

```
1:  $\mathbf{x}^T \sim \mathcal{N}(\mathbf{0}, \mathbf{I})$ 
2: for  $t = T, T-1, \dots, 2, 1$  do
3:    $\epsilon \sim \mathcal{N}(\mathbf{0}, \mathbf{I})$  if  $t > 1$ , else  $\epsilon = \mathbf{0}$ 
4:    $\epsilon_t = g_\phi(\mathbf{x}_t, t)$ 
5:   if  $t > T'$  then
6:      $\hat{\mathbf{x}}_t = \sqrt{\alpha_t} \mathbf{A}^\dagger \mathbf{x}^A + (\mathbf{I} - \mathbf{A}^\dagger \mathbf{A}) \mathbf{x}_t + \mathbf{A}^\dagger \mathbf{A} \sqrt{1 - \alpha_t} \epsilon_t$ 
7:      $\mathbf{x}_{t-1} = \frac{1}{\sqrt{\alpha_t}} (\hat{\mathbf{x}}_t - \frac{1 - \alpha_t}{\sqrt{1 - \alpha_t}} \epsilon_t) + \sigma_t \epsilon$ 
8:   else
9:      $\mathbf{x}_{t-1} = \frac{1}{\sqrt{\alpha_t}} (\mathbf{x}_t - \frac{1 - \alpha_t}{\sqrt{1 - \alpha_t}} \epsilon_t) + \sigma_t \epsilon$ 
10:  end if
11: end for
12: return  $\mathbf{x}_0$ 
```

where \mathbf{x}_t is the noisy image at time step t , which is transformed from the image \mathbf{x}_{t+1} at time step $t+1$. While $\hat{\mathbf{x}}_t$ denotes the approximated image of \mathbf{x}_t based on the range-null decomposition, and we can have $\hat{\mathbf{x}}_t - \mathbf{x}_t = \sqrt{\alpha_t} \mathbf{A}^\dagger \mathbf{A} \mathbf{p}$. The above approximation of \mathbf{x}_t is based on several known factors:

- Since the reverse process begins from T , t is very large at the beginning, and the value of $\sqrt{\alpha_t}$ will be very small, making $\sqrt{\alpha_t} \mathbf{A}^\dagger \mathbf{A} \mathbf{p}$ negligible compared to other terms like $(\mathbf{I} - \mathbf{A}^\dagger \mathbf{A}) \hat{\mathbf{x}}_t$, or $\mathbf{A}^\dagger \mathbf{A} \sqrt{1 - \alpha_t} \epsilon_t$.
- Backdoor attacks are generally stealthy and have much smaller patterns compared to the original images since the attacker wants to minimize the impact on the model’s accuracy on legitimate data while still being able to trigger the backdoor [19]. Thus, compared to \mathbf{x}^A , $\mathbf{A} \mathbf{p}$ can be ignored.
- $\mathbf{A}^\dagger \mathbf{A} \mathbf{p}$ can be further reduced by selecting appropriate image transformation techniques. Since most backdoor attacks are characterized by severe high-frequency artifacts [25], we select average pooling as our transformation method. Average pooling can effectively blur the input images, resulting in the remove of high-frequency information.

Overall, we can have $\hat{\mathbf{x}}_t \approx \mathbf{x}_t$. Therefore, we can modify Equation 10 into the following form:

$$\mathbf{x}_{t-1} = \frac{1}{\sqrt{\alpha_t}} (\hat{\mathbf{x}}_t - \frac{1 - \alpha_t}{\sqrt{1 - \alpha_t}} \epsilon_t) + \sigma_t \epsilon = \frac{1}{\sqrt{\alpha_t}} (\sqrt{\alpha_t} \mathbf{A}^\dagger \mathbf{x}^A + (\mathbf{I} - \mathbf{A}^\dagger \mathbf{A}) \mathbf{x}_t + \mathbf{A}^\dagger \mathbf{A} \sqrt{1 - \alpha_t} \epsilon_t - \frac{1 - \alpha_t}{\sqrt{1 - \alpha_t}} \epsilon_t) + \sigma_t \epsilon, \quad (12)$$

As the reverse process progresses and t becomes smaller, the value of $\sqrt{\alpha_t}$ increases, indicating that the pattern in $\mathbf{A}^\dagger \mathbf{A} \mathbf{p}$ becomes increasingly important and cannot be neglected. To address this issue, we revert to the regular reverse process (see the unguided reverse part in Figure 1) as shown in Equation 5. We believe that the semantic information embedded in \mathbf{x}_t is sufficient to guide the model to generate high-quality images when t is relatively small ($t < T' = \lambda T$), where λ is a hyperparameter to control model change. Furthermore, since the poisoned pattern is typically outside the pre-trained model’s distribution, the last few unguided steps do not generate any trigger patterns on our purified images. We provide our proposed algorithm in Algorithm 1.

3.5 Inference Speed-up

Although Equation 12 can generate high-quality purified images in the zero-shot and black-box settings, it is slow during inference, making it difficult to use for real-world applications. The slow inference speed of DDPM is due to the fact that it requires a large number of steps to generate a single sample. Since each step involves computing the estimated noise and diffusion process, which can be computationally expensive and require improvement.

Therefore, we introduce the denoising diffusion implicit model (DDIM), a recent extension of DDPM that aims to improve its inference speed. Here we modify our reverse process based on the DDIM instead of DDPM. The original DDIM has the reverse process shown below:

$$\mathbf{x}_{t-1} = \sqrt{\bar{\alpha}_{t-1}} \mathbf{x}_{0|t} + \sqrt{1 - \bar{\alpha}_{t-1} - \sigma_t^2} \epsilon_t + \sigma_t \epsilon, \quad (13)$$

Algorithm 2 Zero-shot Image Purification (with DDIM)

Require: Poisoned image \mathbf{x}^P ; linear transformation \mathbf{A} and its pseudo-inverse \mathbf{A}^\dagger ; pre-trained diffusion model g ; hyperparameter λ ; speed-up pace S .

Ensure: $\mathbf{x}^A = \mathbf{A}\mathbf{x}^P$, $T' = \lambda T$

```
1:  $\mathbf{x}^T \sim \mathcal{N}(\mathbf{0}, \mathbf{I})$ 
2: for  $t = T, T - S, \dots, S, 1$  do
3:    $\epsilon \sim \mathcal{N}(\mathbf{0}, \mathbf{I})$  if  $t > 1$ , else  $\epsilon = \mathbf{0}$ 
4:    $\epsilon_t = g_\phi(\mathbf{x}_t, t)$ 
5:   if  $t > T'$  then
6:      $\hat{\mathbf{x}}_t = \sqrt{\bar{\alpha}_t} \mathbf{A}^\dagger \mathbf{x}^A + (\mathbf{I} - \mathbf{A}^\dagger \mathbf{A}) \mathbf{x}_t + \mathbf{A}^\dagger \mathbf{A} \sqrt{1 - \bar{\alpha}_t} \epsilon_t$ 
7:      $\hat{\mathbf{x}}_{0|t} = \frac{1}{\sqrt{\bar{\alpha}_t}} (\hat{\mathbf{x}}_t - \sqrt{1 - \bar{\alpha}_t} \epsilon_t)$ 
8:      $\mathbf{x}_{t-1} = \sqrt{\bar{\alpha}_{t-1}} \hat{\mathbf{x}}_{0|t} + \sqrt{1 - \bar{\alpha}_{t-1} - \sigma_t^2} \epsilon_t + \sigma_t \epsilon$ 
9:   else
10:     $\mathbf{x}_{t-1} = \sqrt{\bar{\alpha}_{t-1}} \mathbf{x}_{0|t} + \sqrt{1 - \bar{\alpha}_{t-1} - \sigma_t^2} \epsilon_t + \sigma_t \epsilon$ 
11:   end if
12: end for
13: return  $\mathbf{x}_0$ 
```

where $\mathbf{x}_{0|t}$ is an estimated image based on the step t observation \mathbf{x}_t and can be calculated using Equation 4. Our modified speed-up reverse process is shown below:

$$\mathbf{x}_{t-1} = \sqrt{\bar{\alpha}_{t-1}} \hat{\mathbf{x}}_{0|t} + \sqrt{1 - \bar{\alpha}_{t-1} - \sigma_t^2} \epsilon_t + \sigma_t \epsilon, \quad (14)$$

where $\hat{\mathbf{x}}_{0|t}$ is also an estimated image based on $\hat{\mathbf{x}}_t$, where we have $\hat{\mathbf{x}}_{0|t} = \frac{1}{\sqrt{\bar{\alpha}_t}} (\hat{\mathbf{x}}_t - \sqrt{1 - \bar{\alpha}_t} \epsilon_t)$.

By applying the above speed-up inference, instead of conducting sampling in thousands of steps, we can sample less than a hundred steps to yield a high-fidelity purified image. The modified algorithm using DDIM is provided in Algorithm 2.

4 Experiments

In this section, we conduct experiments to evaluate the performance of the proposed backdoor defense framework ZIP, in order to answer the following research questions: (1) Does the proposed purification method effectively remove the effects of poisoned triggers? (2) Can the proposed framework successfully defend against various attacks while maintaining high classification accuracy on clean images? and (3) Does our proposed diffusion model recover the semantic information removed by strong transformations?

4.1 Experimental Settings

For defense evaluation, we conducted experiments on three types of backdoor attacks: BadNet [6], Blended [3], and Attack in the physical world (PhysicalBA) [17]. To configure these attack algorithms, we follow the benchmark paper setting [16] and utilize the open-sourced code provided. We evaluated the effectiveness of our defense framework on three datasets: CIFAR-10 [13], GTSRB [23], and Imagenette [10]. Our poisoned classification network was based on ResNet-34 [8].

To implement our proposed purification method, we select average pooling as the linear transformation \mathbf{A} and up-sampling as the pseudo-inverse operation \mathbf{A}^\dagger . We also select a pre-trained diffusion model from [4] that is designed to process images with a fixed size of 256x256 pixels. To ensure that our proposed purification method is applicable to various datasets, we develop a tiling strategy. For images with dimensions smaller than 256x256 pixels, we combine them into a single larger image by tiling them. For example, by tiling 64 images of size 32x32, we can create a 256x256 image. We then apply our purification method to the resulting tiled image, and split the purified image back into the original sizes. For images with dimensions larger than 256x256 pixels, we resize them to 256x256 before applying our method. This tiling strategy enables our defense approach to handle images of various sizes while also significantly increasing the purification speed for small images by processing multiple images simultaneously. Furthermore, we employ the algorithm described in Algorithm 2 to further accelerate the inference process. As a result, we can generate high-quality images in just 20 steps.

To assess the effectiveness of our proposed method, we conduct a comparative evaluation against two baseline approaches, namely ShrinkPad [18] and the Naive Transformation. The former is a state-of-the-art image transformation based defense method that can work on black-box models in the zero-shot setting. While the latter is an image transformation based defense method, where we naively use the transformed images $\mathbf{A}^\dagger \mathbf{x}^A$ as purified images. We apply our purification process and baseline defense methods to all test datasets, and then evaluate the purified/defended test set using poisoned models. In addition to using the clean accuracy (CA) and attack success rate (ASR) metrics to assess the effectiveness of our defense, we introduce a new metric called poisoned accuracy (PA). The PA metric measures the classification performance of the purified attacked samples on the poisoned model. A higher PA value indicates a higher likelihood for the original poisoned samples to be correctly classified despite using an attacked classification neural network.

4.2 Qualitative Results of Purification

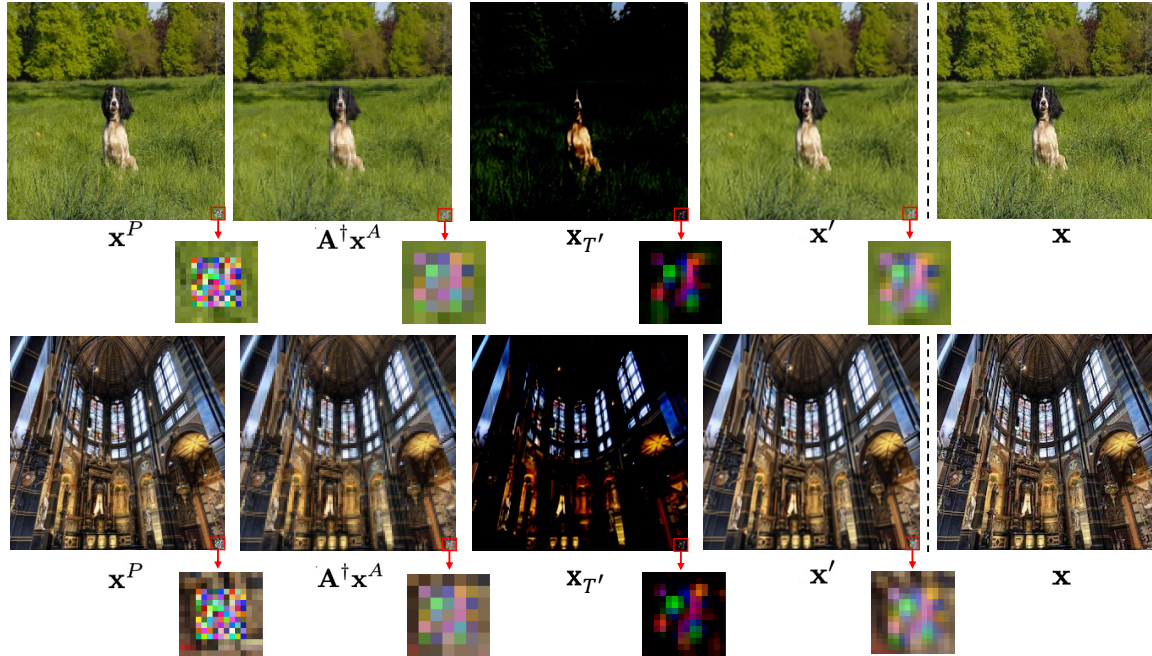
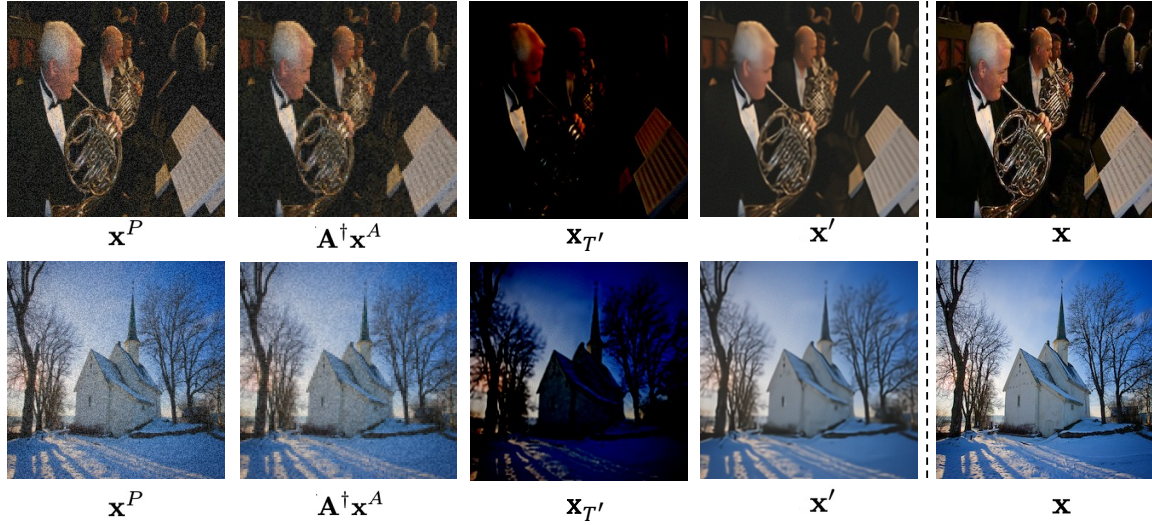


Figure 2: Qualitative results of purification on test images.

To answer research question (1), we conducted qualitative experiments on poisoned images with trigger patterns selected from the BadNet and Blended attack. We applied our purification method to these images. Figure 2 shows examples of poisoned images \mathbf{x}^P and purified image \mathbf{x}' , where the trigger pattern is clearly visible in the poisoned images but has been altered/removed in the purified images. We also demonstrated the transformed image $\mathbf{A}^\dagger \mathbf{x}^A$ and the generated images $\mathbf{x}_{T'}$ from the diffusion model at step T' . We can observe that the transformed images can destruct the trigger pattern, but they also destruct semantic information. We can also find that the generated image $\mathbf{x}_{T'}$ contains sufficient semantic information to guide the diffusion model. Overall, these results demonstrate the effectiveness of our proposed purification method in removing the effect of trigger patterns from images while maintaining semantic information.

4.3 Quantitative Results of Defense

Table 1: The clean accuracy (CA %), the attack success rate (ASR %), and the poisoned accuracy (PA %) of three backdoor defense methods against three kinds of backdoor attacks, including two visible backdoor attacks and one invisible attacks. *None* means the training data is completely clean.

Dataset	Types	No Defense			ShrinkPad			Naive Transformation			ZIP (Ours)		
		CA \uparrow	ASR \downarrow	PA \uparrow	CA \uparrow	ASR \downarrow	PA \uparrow	CA \uparrow	ASR \downarrow	PA \uparrow	CA \uparrow	ASR \downarrow	PA \uparrow
CIFAR-10 (32×32) (10 classes)	None	80.15	—	—	—	—	—	—	—	—	—	—	—
	BadNet	80.57	99.98	10.00	63.67	9.24	62.98	59.13	21.56	54.59	72.57	1.30	70.93
	Blended	80.26	99.96	10.03	58.97	2.28	40.22	55.91	3.04	49.91	74.84	3.29	65.39
	PhysicalBA	94.77	99.99	10.01	93.15	99.95	10.05	54.86	5.88	52.28	81.17	0.86	78.90
	Average	85.20	99.98	10.01	71.93	37.16	37.75	56.63	10.16	52.26	76.19	1.82	71.74
GTSRB (32×32) (43 classes)	None	96.95	—	—	—	—	—	—	—	—	—	—	—
	BadNet	96.53	99.99	5.70	78.33	5.81	78.82	95.98	7.33	95.11	96.25	6.07	96.12
	Blended	96.58	99.89	5.79	76.76	10.54	56.41	93.68	11.07	73.91	96.19	8.78	82.09
	PhysicalBA	96.83	100.00	5.70	97.41	100.00	5.70	91.00	5.53	90.53	95.47	6.26	95.29
	Average	96.65	99.96	5.73	84.17	38.78	46.98	93.55	7.98	86.52	95.97	7.04	91.17
Imagenette (256×256) (10 classes)	None	84.58	—	—	—	—	—	—	—	—	—	—	—
	BadNet	84.99	94.53	14.98	71.23	8.56	70.72	81.47	16.45	79.94	84.48	1.30	84.86
	Blended	86.14	99.85	10.19	74.06	20.63	36.10	78.95	79.41	25.57	82.54	15.43	46.08
	PhysicalBA	90.67	72.94	34.29	90.21	96.81	13.07	84.84	32.40	74.87	88.58	4.78	87.94
	Average	87.27	89.11	19.82	78.50	42.00	39.96	81.75	42.75	60.13	85.20	7.17	72.96

We conducted quantitative experiments to answer research questions (2) and (3), the results of which are presented in Table 1. Our experiments demonstrate the effectiveness of our proposed defense methods in reducing the ASR of three types of attacks across three different datasets. Our approach consistently outperformed the other two baseline methods across most datasets and attack types. For example, on the Imagenette dataset, our method reduces the ASR of the BadNet attack from 94.53% (with no defense) to just 1.3%, with only a 0.51% CA drop. Similarly, on the GTSRB dataset, our approach reduces the success rate of the PhysicalBA attack from 100% (with no defense) to 6.26%, with only a 1.36% CA drop.

Our observations are as follows: (1) Our model successfully defends against various backdoors while maintaining classification accuracy compared to baseline methods. This is because our approach not only uses transformations to create a mismatch between poisoned triggers and poisoned labels, but also uses a diffusion model to recover lost semantic information to ensure accurate classification. (2) Our proposed purification-based method also outperforms the other two methods in a new evaluation metric that we propose, poisoned accuracy (PA), indicating that contaminated samples can still be used for classification even when using an attacked black-box model as the classifier. This demonstrates the robustness of our approach in real-world scenarios. (3) We find that the ShrinkPad method performs poorly on the PhysicalBA attack, which is consistent with the findings in [17]. This is because PhysicalBA attack is specifically designed to evade defense methods such as ShrinkPad [17]. However, our proposed model successfully defends against this attack, demonstrating its superior performance compared to existing defense methods.

5 Related Work: Backdoor Defense

Existing defense methods for black-box backdoor models can be classified into two types. The first type involves training a proxy detection model using a batch of collected clean/poisoned images as input [25, 7, 14]. This detection model distinguishes between clean and poisoned samples by comparing

them with other samples. However, this approach has three limitations. First, the success of the defense depends strongly on the quality [7, 25] and quantity [25, 14] of the collected data. Second, for any new attacks with new trigger patterns, the detection model requires retraining, which can be time consuming. Lastly, when detecting images that contain the trigger pattern, these methods will usually reject poisoned images and avoid performing any further inference on them [7, 25]. Users naturally expect to receive results for all their test samples, so discarding attacked test images is not a viable option, which limits the usefulness of these methods in real-world applications. The second type of defense methods applies strong image transformations on test images before feeding them to the poisoned model for prediction [17]. Strong transformation introduces variations to the input images, creating a mismatch of trigger patterns and poisoned labels, making it more difficult for the poisoned model to recognize the trigger pattern. On the one hand, transformation-based methods can alleviate the limitations of the first type and help users make use of poisoned data. On the other hand, these methods can only defend against static pattern-based attacks. They cannot effectively detect more advanced attacks, such as those with dynamic patterns [17], which limits their application.

6 Conclusion

In this paper, we propose a novel framework for protecting against backdoor attacks under black-box setting. In detail, we first apply a strong transformation on the poisoned image to destroy the trigger pattern, and then utilize a pre-trained diffusion model to recover the removed semantic information removed by the transformation to maintain the fidelity of the purified images. We have conducted experiments to demonstrate the effectiveness of our proposed methods in defending against various backdoor attacks. Our contributions include the development of an effective poisoned image purification method that does not require model internal information or any training samples. Our method enables end-users to utilize full test samples without discarding any, even when using an attacked classification model. In summary, our framework provides a promising solution for defending against backdoor attacks on black-box models and has the potential to enhance the security and robustness of machine learning systems. Further research and development in this area can build upon our proposed methods and expand the scope of their application.

References

- [1] Amazon SageMaker - Build, Train, and Deploy Machine Learning Models at Scale. <https://aws.amazon.com/sagemaker/>. Accessed: March 20, 2023.
- [2] Azure Machine Learning - Use an enterprise-grade service for the end-to-end machine learning lifecycle. <https://azure.microsoft.com/en-us/products/machine-learning/>. Accessed: March 20, 2023.
- [3] Xinyun Chen, Chang Liu, Bo Li, Kimberly Lu, and Dawn Song. Targeted backdoor attacks on deep learning systems using data poisoning. *arXiv preprint arXiv:1712.05526*, 2017.
- [4] Prafulla Dhariwal and Alexander Nichol. Diffusion models beat gans on image synthesis. *Advances in Neural Information Processing Systems*, 34:8780–8794, 2021.
- [5] Yinpeng Dong, Xiao Yang, Zhijie Deng, Tianyu Pang, Zihao Xiao, Hang Su, and Jun Zhu. Black-box detection of backdoor attacks with limited information and data. In *Proceedings of the IEEE/CVF International Conference on Computer Vision*, pages 16482–16491, 2021.
- [6] Tianyu Gu, Brendan Dolan-Gavitt, and Siddharth Garg. Badnets: Identifying vulnerabilities in the machine learning model supply chain. *arXiv preprint arXiv:1708.06733*, 2017.
- [7] Junfeng Guo, Ang Li, and Cong Liu. Aeva: Black-box backdoor detection using adversarial extreme value analysis. *arXiv preprint arXiv:2110.14880*, 2021.
- [8] Kaiming He, Xiangyu Zhang, Shaoqing Ren, and Jian Sun. Deep residual learning for image recognition. In *Proceedings of the IEEE conference on computer vision and pattern recognition*, pages 770–778, 2016.
- [9] Jonathan Ho, Ajay Jain, and Pieter Abbeel. Denoising diffusion probabilistic models. *Advances in Neural Information Processing Systems*, 33:6840–6851, 2020.

- [10] Jeremy Howard. Imagenette. <https://github.com/fastai/imagenette>, 2019.
- [11] Patanjali Kashyap. *Machine learning for decision makers: Cognitive computing fundamentals for better decision making*. Springer, 2017.
- [12] Bahjat Kavar, Michael Elad, Stefano Ermon, and Jiaming Song. Denoising diffusion restoration models. *arXiv preprint arXiv:2201.11793*, 2022.
- [13] Alex Krizhevsky, Geoffrey Hinton, et al. Learning multiple layers of features from tiny images. 2009.
- [14] Yige Li, Xixiang Lyu, Nodens Koren, Lingjuan Lyu, Bo Li, and Xingjun Ma. Anti-backdoor learning: Training clean models on poisoned data. *Advances in Neural Information Processing Systems*, 34:14900–14912, 2021.
- [15] Yiming Li, Yong Jiang, Zhifeng Li, and Shu-Tao Xia. Backdoor learning: A survey. *IEEE Transactions on Neural Networks and Learning Systems*, 2022.
- [16] Yiming Li, Mengxi Ya, Yang Bai, Yong Jiang, and Shu-Tao Xia. Backdoorbox: A python toolbox for backdoor learning. *arXiv preprint arXiv:2302.01762*, 2023.
- [17] Yiming Li, Tongqing Zhai, Yong Jiang, Zhifeng Li, and Shu-Tao Xia. Backdoor attack in the physical world. *arXiv preprint arXiv:2104.02361*, 2021.
- [18] Yiming Li, Tongqing Zhai, Baoyuan Wu, Yong Jiang, Zhifeng Li, and Shutao Xia. Rethinking the trigger of backdoor attack. *arXiv preprint arXiv:2004.04692*, 2020.
- [19] Anh Nguyen and Anh Tran. Wanet—imperceptible warping-based backdoor attack. *arXiv preprint arXiv:2102.10369*, 2021.
- [20] Ziad Obermeyer and Ezekiel J Emanuel. Predicting the future—big data, machine learning, and clinical medicine. *The New England journal of medicine*, 375(13):1216, 2016.
- [21] Han Qiu, Yi Zeng, Shangwei Guo, Tianwei Zhang, Meikang Qiu, and Bhavani Thuraisingham. Deepsweep: An evaluation framework for mitigating dnn backdoor attacks using data augmentation. In *Proceedings of the 2021 ACM Asia Conference on Computer and Communications Security*, pages 363–377, 2021.
- [22] Johannes Schwab, Stephan Antholzer, and Markus Haltmeier. Deep null space learning for inverse problems: convergence analysis and rates. *Inverse Problems*, 35(2):025008, 2019.
- [23] Johannes Stallkamp, Marc Schlipsing, Jan Salmen, and Christian Igel. Man vs. computer: Benchmarking machine learning algorithms for traffic sign recognition. *Neural networks*, 32:323–332, 2012.
- [24] Yinhuai Wang, Jiwen Yu, and Jian Zhang. Zero-shot image restoration using denoising diffusion null-space model. *arXiv preprint arXiv:2212.00490*, 2022.
- [25] Yi Zeng, Won Park, Z Morley Mao, and Ruoxi Jia. Rethinking the backdoor attacks’ triggers: A frequency perspective. In *Proceedings of the IEEE/CVF International Conference on Computer Vision*, pages 16473–16481, 2021.
- [26] Yi Zeng, Han Qiu, Shangwei Guo, Tianwei Zhang, Meikang Qiu, and Bhavani Thuraisingham. Deepsweep: An evaluation framework for mitigating dnn backdoor attacks using data augmentation. *arXiv e-prints*, pages arXiv–2012, 2020.
- [27] Tao Zhang, Qing Li, Chang-shui Zhang, Hua-wei Liang, Ping Li, Tian-miao Wang, Shuo Li, Yun-long Zhu, and Cheng Wu. Current trends in the development of intelligent unmanned autonomous systems. *Frontiers of information technology & electronic engineering*, 18:68–85, 2017.